

Micromagnetic approach to exchange bias—A new look at an old problem

J. Dubowik

*Institute of Molecular Physics, Polish Academy of Physics,
M. Smoluchowskiego 17, PL-60-179, Poznań, Poland*

I. Gościańska

*Faculty of Physics, A. Mickiewicz University,
Umultowska 85, PL-61-614, Poznań, Poland*

(Dated: August 2, 2018)

Abstract

We present a micromagnetic approach to the exchange bias (EB) in ferromagnetic (FM)/antiferromagnetic (AFM) thin film systems with a small number of irreversible interfacial magnetic moments. We express the exchange bias field H_{EB} in terms of the fundamental micromagnetic length scale of FM—the exchange length l_{ex} . The benefit from this approach is a better separation of the factor related to the FM layer from the factor related to the FM/AFM coupling at interfaces. Using this approach we estimate the upper limit of H_{EB} in real FM/AFM systems.

PACS numbers: 75.30.Gw, 75.30.Et, 75.60.Jk

I. INTRODUCTION

The coupling between a ferromagnet (FM) and an antiferromagnet (AFM) that is set up on field cooling from temperatures above the Néel temperature of the AFM results in an exchange bias (EB).¹ However, it seems that we do not yet have a general and compact micromagnetic description of EB in spite of a number of numerical simulations^{2–4} and models.^{5,6} In this respect, three main points need to be emphasized. (*i*) In numerous proposed mesoscopic and microscopic models of EB^{5,6}, the master formula for the unidirectional anisotropy field H_{EB} (the exchange bias field) is

$$H_{EB} = \frac{J_{EB}}{M t_{FM}}, \quad (1)$$

where J_{EB} is the interfacial exchange bias energy and t_{FM} is the thickness of the FM layer with magnetization M . Equation (1) represents a micromagnetic relation expressing the equilibrium between the exchange bias energy density J_{EB}/t_{FM} and the Zeeman energy.¹ The main problem in this relation is J_{EB} , which is generally ill-defined, so that we do not know how it is determined by the fundamental parameters of a ferromagnet, taking into account the peculiarities of the interface structure, and of the antiferromagnet. For example, if we arbitrarily suppose that J_{EB} is determined exclusively by the AFM, then, in accordance with Eq. (1), H_{EB} should somehow decrease for EB systems with FM of a high magnetization (e.g., Co). However, we will show in Sec. III that the tendency is in general quite opposite. A ferromagnet with a high magnetization and a high exchange stiffness gives usually the highest H_{EB} . (*ii*) An important step forward in explaining the magnitude of the EB has been done by Stöehr's group, who, using x-ray magnetic circular dichroism, showed that EB is produced by a small ($\approx 0.04 = 4\%$) number of irreversible AFM spins.^{7,8} Therefore, a spin structure at an FM/AFM interface consists of two groups. First, the uncompensated AFM spins—weakly coupled to the rest of the AFM spin lattice so that they can rotate. Second, the irreversible spins—a small fraction of uncompensated spins that are tightly coupled to the AFM spin lattice. Hence, a reduction factor ϵ equal to the fraction of irreversible spins should be taken into account if Eq. (1) is to explain the experimental data. (*iii*) In FM/AFM bilayers, the coercive field H_C of the FM undergoes a substantial increase by a factor of 10–20 in comparison with a single FM film due to an anisotropy $\langle K \rangle$ imposed on the FM by the AFM's uncompensated spins.⁵ However, after inspecting a large number of available experimental data,^{9,10} it appears that the saturation

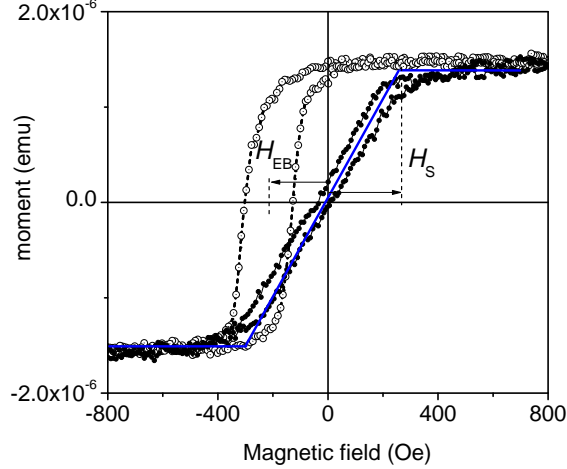


FIG. 1. Magnetization (M) versus magnetic field (H) curves of a sample with the following layer structure: Si (substrate)/IrMn(20 nm)/Co(4 nm)/IrMn(20 nm). Dashed line and open circles: field parallel to the exchange bias field. Full circles and blue lines: field perpendicular to the exchange bias field. The film was prepared under the same conditions as described in Ref. 11

field H_S (measured in the hard direction) of the FM coupled to an AFM is a more reliable quantity than H_C measured in the easy direction. Figure 1 serves as a typical example showing that H_S is of the order of H_{EB} . Therefore, the uniaxial anisotropy field H_S is

$$H_S = \frac{2 \langle K \rangle}{M}. \quad (2)$$

The aim of the present paper is to express Eq. (1) in a more fundamental form involving the micromagnetic characteristics of the FM. It should be stressed that by using magnetic measurements of FM/AFM systems with EB, we can only determine the magnetic properties of the FM. Nevertheless, looking from the FM side, we can argue about an interaction between the FM and the AFM. We shall concentrate on the most important aspects of EB, namely the main factors that determine the values of H_{EB} and J_{EB} . In particular, we shall determine the role of the FM layer and we shall look for an FM/AFM system that fulfils the requirements of an almost ideal EB effect.

II. MODEL

Three quantities describe the micromagnetism of ferromagnets: the magnetization M , the magnetic anisotropy K , and the exchange stiffness constant A . Since the exchange in-

interactions are relevant for a long range spin ordering, we postulate that the last quantity is mainly responsible for interactions between the FM and AFM layers. In the first approximation, let us assume that an FM/AFM interface is ideal, so that the interfacial spins are fully coupled. It can be easily derived from the definition of the exchange interaction in the Heisenberg approach that J_{EB} can be approximated by $2\langle A \rangle/\xi$, where $\langle A \rangle$ is the average exchange stiffness of an FM layer within an interface region with a thickness ξ of the order of the lattice parameter.² Hence Eq. (1) takes the form

$$H_{EB} = \frac{2\langle A \rangle}{M \xi t_{FM}}. \quad (3)$$

Equivalently, the micromagnetic characteristics of an FM can be expressed in terms of the exchange length l_{ex} and the exchange correlation length l_{cor} (domain wall parameter) defined as

$$l_{ex} = \sqrt{(A/2\pi M^2)}, \quad (4)$$

$$l_{cor} = \sqrt{(A/K)},$$

respectively. Both l_{ex} and l_{cor} are the fundamental length scales that control the behavior of magnetic materials and are relevant for the description of an inhomogeneous orientation of the spin structure.¹² In Tab. I, we gathered the values of the magnetic polarization $4\pi M$ and the exchange stiffness A necessary for the estimation of l_{ex} for the typical soft magnetic materials, some Heusler alloys, and magnetite. The values of l_{ex} are within the range of $3 - 8 \times 10^{-7}$ cm = 3–8 nm, while l_{cor} (of the order of the Bloch wall thickness) varies considerably from $l_{cor} \approx 1$ nm in hard magnetic materials to over 100 nm in soft ferromagnets.¹² The spin-wave stiffness $D = 2g\mu_B A/M$ is also included for comparison, since both A and D are frequently used to describe the stiffness of exchange interactions. g is the Landé g-factor and μ_B is the Bohr magneton.

By multiplying and dividing Eq. (3) by $4\pi M$, we can express it in a different way:

$$H_{EB} = 4\pi M \frac{\langle A \rangle}{2\pi M^2} \frac{1}{\xi t_{FM}} = 4\pi M \frac{\langle l_{ex} \rangle^2}{\xi t_{FM}}, \quad (5)$$

where $\langle l_{ex} \rangle$ denotes an averaged exchange length within the interface region. For a typical value of $l_{ex} = 5$ nm (see Tab. I), Eq. (5) leads to an unrealistically high value of $H_{EB} \approx 170$ kOe if we assume typical values for $4\pi M \approx 10$ kG, $\xi \approx 3 \times 10^{-8}$ cm, and $t_{FM} = l_{ex}$. The

TABLE I. Basic magnetic parameters of ferromagnetic *3-d* metals, typical soft magnetic alloys, some Heusler alloys and magnetite (Fe_3O_4): the demagnetizing field $4\pi M$, the exchange stiffness constant A , the spin-wave stiffness D , the exchange length l_{ex} , and the product of demagnetizing field and the square of exchange length.

Material	$4\pi M$ (kOe)	A ($\mu\text{erg}/\text{cm}$)	D (meV nm ²)	l_{ex} (nm)	$4\pi M l_{ex}^2$ (10 ⁹ Oe cm ²)
Fe	21.4 ^a	2.0 ^b	2.8	3.3	2.3
Co	18.1 ^a	2.5 ^b	4.5	4.4	3.5
Ni	6.1 ^a	0.8 ^b	4.5	7.6	3.5
Ni ₈₀ Fe ₂₀	10.0 ^a	1.0 ^b	2.5	5.0	2.5
Co ₄₇ Fe ₅₃	17.0 ^c	5.9 ^c	8.0	7.2	8.7
Co ₂ FeSi	14.1 ^d	3.2 ^d	7.0	6.4	5.7
Co ₂ MnSn	9.9 ^e	0.6 ^e	2.0	3.9	1.5
Ni ₂ MnSn	5.1 ^f	0.1 ^f	0.4	2.6	0.3
Fe ₃ O ₄ ^h	5.9 ^g	0.7 ^g	5.0	7.1	3.0

^a from Ref. 13.

^b from Ref. 14.

^c from Ref. 15.

^d from Ref. 16.

^e from Ref. 17.

^f from Ref. 18.

^g from Ref. 19.

^h All data are representative for room temperature except that of magnetite, which is at 5 K.

comment (*ii*) implies that $\langle A \rangle$ and $\langle l_{ex} \rangle$ are to some extent weakened by the low number of the pinned spins. Let us inspect the impact of the low number of the irreversible spins on $\langle A \rangle$ more closely. If we imagine the interface shown in Fig. 2 with the spins (marked by circles) pinned to the rest of the AFM (marked by shaded area), we can see that they are exchange-coupled with equal numbers ϵ of FM spins. Therefore,

$$\langle A \rangle \approx \frac{I \epsilon S_{FM} \epsilon S_{AFM}}{a} \approx \epsilon^2 A, \quad (6)$$

where I is the exchange integral. S_{FM} and S_{AFM} are the FM and AFM spins, respectively. Here we assume that the EB systems exhibit negative bias, so that the FM spins and

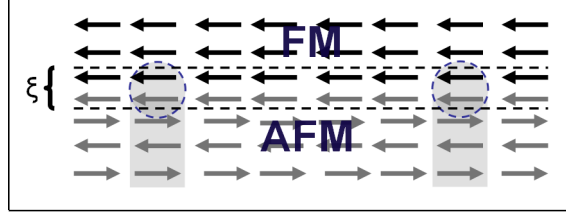


FIG. 2. Schematic diagram of the ferromagnet/antiferromagnet (FM/AFM) interface of thickness ξ with uncompensated spins and the spins (marked by dashed circles) pinned to the AFM spin lattice (shaded area).

irreversible AFM spins are aligned in the same direction ($I > 0$).⁸ Hence, an EB for a realistic interface with a low number of irreversible spins can be expressed by

$$H_{EB} = 4\pi M l_{ex}^2 \frac{\epsilon^2}{\xi t_{FM}} \quad (7)$$

with the product of $4\pi M l_{ex}^2$ as the leading factor. From Tab. I one can see that the leading factor is highest for the Co-Fe alloy and, unexpectedly, for the Co_2FeSi Heusler alloy, while it does not vary much for 3-*d* metals and Ni-Fe. It is easy to show that an ϵ on the order of a few percent provides a realistic value of $H_{EB} \approx 200$ Oe ($\epsilon = 0.015$), as is shown in Fig. 1, for example, and in agreement with other experimental data (see, for example Ref. 5 and references therein). The expression $\langle l_{ex} \rangle = \epsilon l_{ex}$ can be regarded as an effective exchange length in FM due to the low number of irreversible AFM spins. Note, however, that $\langle l_{ex} \rangle$ is on the order of only 0.1 nm if $\epsilon = 0.04$. This is a remarkably small value since, by definition, the exchange length is the length below which atomic exchange interactions dominate over typical magnetostatic fields.¹²

Accordingly, the interfacial exchange bias energy J_{EB} is expressed by

$$J_{EB} = 2\pi M^2 \left(\frac{2l_{ex}^2 \epsilon^2}{\xi} \right), \quad (8)$$

where the second factor in parentheses has the dimension of length scale of 200 nm if $\epsilon = 1$ so that J_{EB} would take a huge value of 50–150 erg/cm². However, since J_{EB} must be less than $K_{AFM} \times t_{AFM}$,¹ the upper limit of J_{EB} is less than 10 erg/cm² if $K_{AFM} \approx 10^7$ erg/cm³ and $t_{AFM} \approx 5$ nm (a typical critical value of AFM thickness).²⁰ It is noteworthy that if $\epsilon = 0.35$ and 0.04, J_{EB} would be 10–4 and 0.4–0.1 erg/cm², respectively.

III. DISCUSSION

The lowest limit of J_{EB} of 0.1–0.4 erg/cm² is worth comment. Since research into EB encompasses a huge number of papers, we can draw useful conclusions on the average exchange bias energy J_{EB} using simple statistics for a large number of experimental data under the assumption that each experiment is of equal significance. A collection of tabulated data gathered by Coehoorn²⁰ is an invaluable database. We gathered the distribution of the values of J_{EB} (taken from Tab. 13 in Ref. 20) in the form of histograms as shown in Fig. 3. It is clearly seen that both for Ni-Fe and Co-Fe layers in contact with various metallic random substitutional fcc-type AFM alloys, the distributions of the data have the shape of a normal distribution even though the width of the histogram for the Co-Fe data is four times higher than that of the Ni-Fe data. Most important, however, is that the mean value of J_{EB} is 0.1 and 0.25 erg/cm² for Ni-Fe and Co-Fe, respectively. If we estimate the values of J_{EB} making use of Eq. (8) assuming $\epsilon = 0.04$, we unexpectedly arrive at $J_{EB} = 0.11$ and 0.24 erg/cm², nearly the same as the mean values evaluated from the histograms for Ni-Fe and Co-Fe, respectively. For the calculations, we took the appropriate data from Tab. I and $\xi = 0.3$ and 0.25 nm for permalloy and Co, respectively. The remarkable agreement between the experimental and calculated values of J_{EB} may seem a coincidence, but it may also suggest that the assumed ratio of the irreversible pinned spins of just a few percent is typical of metallic FM/AFM systems. One of the highest values of J_{EB} ever measured for metallic FM/AFM bilayers (with a high $4\pi M l_{ex}^2$ factor) is 1.3 erg/cm² for Co₇₀Fe₃₀ in contact with a highly L1₂ ordered Mn₃Ir phase.²¹ A rough estimate employing Eq. (8) suggests that such a “giant” value is achieved for a merely twofold increase in ϵ to 0.08–0.09.

Therefore, the FM/AFM systems behave as if a specific localized exchange coupling between ϵ fraction of FM spins and an equal fraction of AFM irreversible spins were blurred in a delocalized “sea” of FM interacting spins. In this aspect, EB can be regarded as a perturbation in the exchange energy of the FM in contact with AFM.

Still, Eq. (7) describes an idealized case of the exchange bias. In reality, in most cases both the FM and the AFM have a large number of defects: they consist of grains on a nanometer scale with grain boundaries, etc. Nevertheless, Eq. (7) captures the most important material and interface characteristics that determine the order of magnitude of the exchange bias on the nanoscale. The most characteristic in Eq. (7) is that the factor

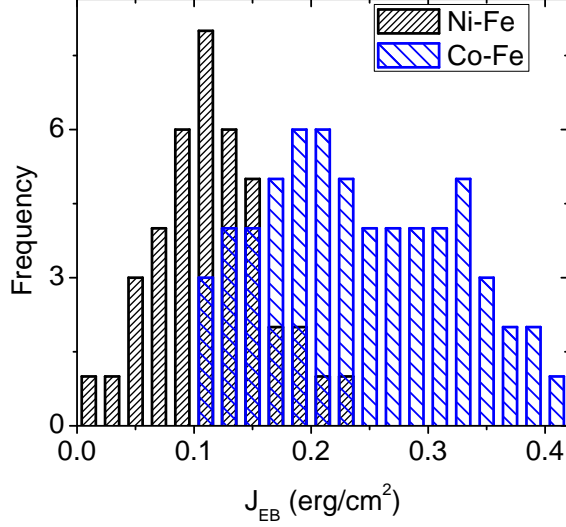


FIG. 3. Histograms showing distribution of the experimental values of J_{EB} taken from Tab. 13 in Ref. 20. The histograms show distribution of the data for Ni-Fe ($\text{Ni}_{80}\text{Fe}_{20}$) and for Co-Fe films ($\text{Co}_{90}\text{Fe}_{10}$), respectively. Frequency has the meaning of the number of data falling in a bin of J_{EB}

$4\pi M l_{ex}^2$ depends exclusively on the FM (due to our assumption that the interface coupling between the irreversible AFM spins and the FM spins is positive), while the factor ϵ^2 depends mostly on the AFM (its anisotropy) and the quality of the interface.

By applying the same transformation to Eq. (2) as to Eq. (5), we have

$$H_S = 4\pi M \frac{\langle K \rangle}{2\pi M^2} \frac{\epsilon^2 A}{\epsilon^2 A} = 4\pi M l_{ex}^2 \frac{1}{l_{cor}^2}, \quad (9)$$

which has the same symmetrical form as Eq. (7) with l_{cor}^2 in the denominator. It is characteristic that the factor ϵ^2 is absent. For a typical value of $H_S = 200$ Oe in Fig. 1, Eq. (9) leads to $l_{cor} = 32$ nm.

The presence of both l_{ex} and l_{cor} in Eqs (7) and (9) may be linked with an inhomogeneous spin structure of the FM and suggests the formation of a magnetization twisting. Such a magnetization twisting was analyzed about 50 years ago by Aharoni *et al.*²² They considered a ferromagnetic slab, infinite in the x and y directions and of width $2t_{FM}$. At $t = z/t_{FM} = \pm 1$, the spins are assumed to be held in the x direction by the exchange coupling with the AFM and expressed with appropriate boundary conditions. Let an external field H be applied in the x direction. The easiest mode for magnetization changes is evidently rotation of the spins in the xy plane. The functions which minimize the energy of such a system are

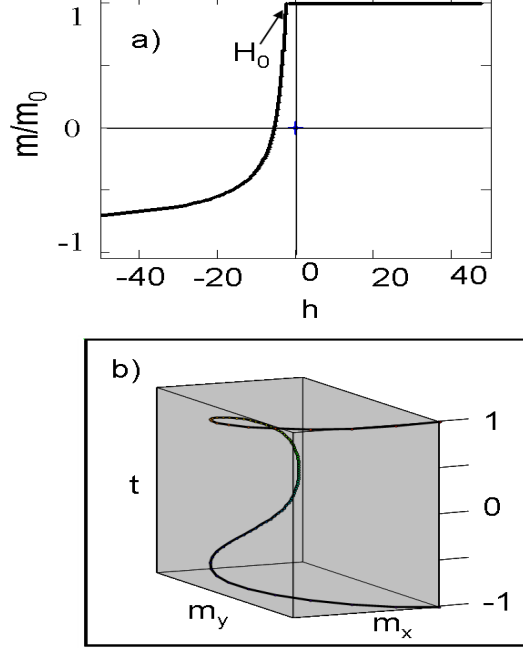


FIG. 4. (a) Asymmetrical dependence of reduced magnetization m versus reduced magnetic field h applied opposite to the pinning direction. (b) Twisting of the magnetization vector defined as $\vec{m} = \vec{i} \cos \Theta(t) + \vec{j} \sin \Theta(t)$ with the distance between two FM/AFM interfaces for $h = 0.5$. The magnetization is fully pinned at $t = \pm 1$.

the solutions of the Euler equation

$$\frac{d^2 \Theta}{dt^2} - \frac{h}{(t_{FM}/l_{ex})^2} \sin \Theta = 0, \quad (10)$$

with the boundary conditions $\Theta'(0) = 0$, $\Theta(\pm 1) = 0$ and with $h = H/4\pi M$. The solution of Eq. (10) is expressed in terms of the complete elliptic integral of the first kind K_C

$$\Theta(t) = 2 \arcsin(k \operatorname{sn}[(1-t)K_C(k), k]), \quad (11)$$

where sn is the sine amplitude function and k is “hidden” in the relation $-h = K_C^2(k)/(t_{FM}/l_{ex})^2$. This solution leads to a strongly asymmetric magnetization reversal curve as shown in Fig. 4 (a), which saturates at $-h \approx \infty$. This important approach to EB has not attracted much attention except in some old papers.²³ Similar asymmetric magnetization reversals have been recently observed in Ni/FeF₂ bilayers and interpreted as originating from the intrinsic broken symmetry of the system, which results in local incomplete domain walls parallel to the interface (i.e., the magnetization twisting) in reversal to negative saturation of the FM.³

The twisting of the magnetization vector shown in Fig. 4 (b) comes from the boundary conditions stating that the magnetization is fully “free” at the center of the FM layer and fully “pinned” at the two FM/AFM interfaces.

As is seen in Fig. 4 (a), the magnetization starts twisting above a certain field $h > (\pi/2)^2/(t_{FM}/l_{ex})^2$. Hence,

$$H_0 = 4\pi M l_{ex}^2 \frac{(\pi/2)^2}{t_{FM}^2}. \quad (12)$$

Equation (12) describes the magnitude of the exchange bias field for an ideal FM/AFM system without uniaxial anisotropy imposed by AFM but with fully irreversible spins at the interfaces. The similarity between Eq. (12) and Eq. (7) is striking in that the factor $(\pi/2)^2/t_{FM}^2$ is purely geometrical. If we equate H_{EB} with H_0 (Eq. (7) to Eq. (12)) in order to estimate the maximal value that ϵ can achieve for the ideal pinning described by the boundary conditions, we obtain

$$\epsilon_{max}^2 = (\pi/2)^2 \frac{\xi}{t_{FM}}. \quad (13)$$

For typical values $\xi \approx 0.3$ nm and $t_{FM} \approx l_{ex} \approx 5 - 10$ nm, $\epsilon^2 \approx 0.15 - 0.075$. As a result 38%–27% of the irreversible AFM spins would produce the highest possible values that H_{EB} (J_{EB}) can achieve, i.e., 25–12 kOe (6–3 erg/cm²). Hence, we come to the conclusion that the highest value that ϵ can attain is (38%–27%) is just due to the formation of an incomplete domain wall (i.e., magnetization twisting). In reality, however, AFM is polycrystalline and defected, so that these values are overestimated.⁴

It appears that among a large number of FM/AFM systems all-oxide Fe₃O₄/CoO epitaxial bilayers nearly satisfy the requirements of ideal pinning with $J_{EB} = 2.1$ erg/cm²—the value is only about 8 times smaller than the exchange biasing estimated according to the Meiklejohn–Bean model.^{19,24} J_{EB} estimated from Eq. (8) with $\epsilon^2 = 0.13$ (i.e., $\approx 1/8$) and $\xi \approx 0.8$ nm (lattice parameter of Fe₃O₄) yields $J_{EB} = 2.04$ erg/cm², which justifies the [100] oriented Fe₃O₄/CoO bilayer system’s being very close to the straightforward idea concerning the micromagnetic approach. It is noteworthy that polarized neutron reflectivity measurements of similar Fe₃O₄/NiO multilayers have provided evidence of domain-wall formation (magnetization twisting) in the exchange-biased state but within the ferromagnetic, rather than the AFM, layer.²⁵ A question may be posed: why is the EB the highest in all-oxide FM/AFM systems? Neglecting the complex interplay between the microstructure of the

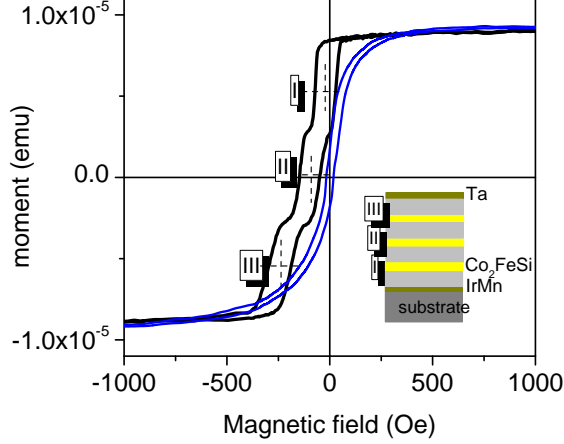


FIG. 5. Hysteresis loops of $[\text{Ta } 5 \text{ nm}/(\text{IrMn } 20 \text{ nm}/\text{Co}_2\text{FeSi } 10 \text{ nm}) \times 3/ \text{IrMn } 20 \text{ nm}/ \text{Ta } 5 \text{ nm}]$ multilayer taken with the magnetic field applied parallel (black) and perpendicular (blue) to H_{EB} direction, respectively. The inset shows the multilayer structure consisting of a stack of IrMn (gray)/ Co_2FeSi (yellow)/IrMn three-layers.

AFM layer and the FM/AFM interface, it seems that superexchange coupling via the intervening p-orbitals of the oxygen atoms plays a leading role. The coupling, between the magnetic ions with half-occupied orbitals (Fe^{2+} and Co^{2+}) through the intermediary oxygen ion, of the superexchange is indirect (the magnetic ions are of 0.4 nm apart) and strongly antiferromagnetic. What seems even more important, is that both oxide lattices are based on an approximately close-packed lattice of oxygen ions with Co^{2+} and Fe^{3+} in tetrahedral or octahedral (Fe^{3+} and Fe^{2+}) interstitial.²⁴ This feature makes $\text{Fe}_3\text{O}_4/\text{CoO}$ epitaxial bilayers a model system to study EB.¹⁹ In contrast, in all-metallic FM/AFM systems, the exchange coupling between the FM and AFM species is direct, so that any change in ordering at the interfaces results in a frustration of exchange interactions.²⁶

Now we can understand why in most of the FM/AFM all-metallic thin film systems the EB field is of the order of 100–400 Oe. As seen in Tab. I, the product $4\pi M l_{ex}^2$ does not differ much among most of the soft FM materials. Therefore, any enhancement of the EB relies mainly on increasing ϵ . We have little room for manoeuvre except to increase ϵ by some technological trick like, for example, dusting the interfaces with ultrathin Co or Mn layers^{11,27} or a proper setting AFM in a magnetic field.⁵ Specifically, ϵ determines the quality of setting AFM on cooling from $T > T_N$.²⁸ A spectacular example of such a gradual improvement in EB is observed in a Ta 5/(IrMn 20/ Co_2FeSi 10) \times 3/ IrMn 20/ Ta 5 multilayer annealed

at 400°C for 15 min. and field cooled to room temperature (Fig. 5). The details of the sample preparation can be found in Ref. 11. As seen in Fig. 5, the hysteresis loop (black) taken with the magnetic field parallel to the exchange bias consists of three loops related to the subsequent Co layers in the stack. These three loops, of equal heights and nearly equal coercive field of ~ 50 Oe, are shifted along the field axis by H_{EB} of 20, 72 and 235 Oe for the first (I), second (II) and third (III) Co layer, respectively. Simultaneously, in accordance with the discussion of Eq. (9), the estimated value of H_S is 150 Oe (see Fig. 5, hysteresis taken with a magnetic field applied perpendicular to H_{EB} direction). It has been confirmed (see Ref. 11 for details) with a magneto-optical Kerr magnetometer that the upper (III) Co layer has the highest H_{EB} . A simple estimate employing Eq. (7) using the data from Tab. I for Co_2FeSi gives the values of ϵ of 0.01, 0.02, and 0.05 for the layers I, II, and III, respectively. As was discussed above, ϵ depends on the interface quality and on the anisotropy of the AFM layer. Since the interfaces in the stack should not differ much, the increase in anisotropy seems to be responsible for these slight changes in ϵ . We have proven with x-ray diffraction measurements (see Ref. 11) that the grain size of IrMn increases as the subsequent layers are deposited from the substrate, so that the increase in AFM anisotropy is justified. However, in view of our discussion, we do not expect that ϵ can exceed the values of several percent in the case of all-metallic FM/AFM systems.

IV. SUMMARY

In summary, we have shown that the exchange bias resulting from a coupling between FM and AFM layers can be described in terms of a rough micromagnetic approach, which seems to capture the essential characteristics of the exchange bias. Specifically, we showed that the interfacial interactions involved between the FM and the AM reduce to a geometrical problem with the fundamental micromagnetic length scale being the exchange length l_{ex} . The model identifies the range of the exchange bias field H_{EB} (exchange bias energy J_{EB}) compatible with those observed in experiment. Using the model, we proved that the highest effective number of irreversible spins is lower than $\sim 30\%$ – 40% .

¹ W. H. Meiklejohn and C. P. Bean, Phys. Rev. **102**, 1413 (1956).

- ² D. Süß, *Micromagnetic simulations of antiferro- and ferromagnetic structures for magnetic recording*, Ph.D. thesis, Wien University, Austria (2002).
- ³ Z.-P. Li, O. Petraciê, R. Morales, J. Olamit, X. Batlle, K. Liu, and I. K. Schuller, *Phys. Rev. Lett.* **96**, 217205 (2006).
- ⁴ M. Fecioru-Morariu, U. Nowak, and G. Güntherodt, in *Magnetic properties of antiferromagnetic oxide materials*, edited by L. Dúo, M. Finazzi, and F. Ciccacci (Wiley-VCH, 2010) Chap. 5.
- ⁵ J. Nogues and I. K. Schuller, *J. Magn. Magn. Mater.* **192**, 203 (1999).
- ⁶ A.E. Berkowitz and K. Takano, *J. Magn. Magn. Mater.* **200**, 552 (1999).
- ⁷ H. Ohldag, T. J. Regan, J. Stöhr, A. Scholl, F. Nolting, J. Luening, C. Stamm, S. Anders, and R. L. White, *Phys. Rev. Lett.* **87**, 247201 (2001).
- ⁸ J. Stöhr and H. C. Siegmann, *Magnetism from fundamentals to nanoscale dynamics*, Series: Springer Series in Solid-State Sciences, Vol. 152 (Springer, Berlin, 2006) Section 10, pp. 100–119.
- ⁹ A. Kohn, J. Dean, A. Kovacs, A. Zeltser, M. J. Carey, D. Geiger, G. Hrkac, T. Schrefl, and D. Allwood, *J. Appl. Phys.* **109** (2011).
- ¹⁰ A. Harres and J. Geshev, *J. Physics.: Condens. Matter* **24**, 326004 (2012).
- ¹¹ J. Dubowik, I. Gościańska, K. Załęski, H. Głowiński, Y. Kudryavtsev, and A. Ehresmann, *J. Appl. Phys.* **113**, 193907 (2013).
- ¹² R. Skomski, *J. Phys.: Condens. Matter* **15**, R841 (2003).
- ¹³ R. O’Handley, *Modern Magnetic Materials: Principles and Applications* (Wiley, 1999).
- ¹⁴ Z. Frait and D. Fraitova, in *Modern problems in condensed matter sciences*, Spin waves and magnetic excitations, Vol. 22.2, edited by A. S. Borovik-Romanov and S. K. Sinha (North-Holland, Amsterdam, 1988) Section 1, pp. 1–65.
- ¹⁵ X. Liu, R. Sooryakumar, C. J. Gutierrez, and G. A. Prinz, *J. Appl. Phys.* **75**, 7021 (1994).
- ¹⁶ S. Trudel, O. Gaier, J. Hamrle, and B. Hillebrands, *J. Phys. D: Applied Physics* **43**, 193001 (2010).
- ¹⁷ R. Yilgin, S. Kazan, B. Rameev, B. Aktas, and K. Westerholt, *J. Phys.: Conf. Series* **153**, 012068 (2009).
- ¹⁸ J. Dubowik, I. Gościańska, K. Załęski, H. Głowiński, A. Ehresmann, G. Kakazei, and S. A. Bunayev, *Acta Phys. Polon. A* **121**, 1121 (2013).

- ¹⁹ P. J. van der Zaag, A. R. Ball, , L. F. Feiner, R. M. Wolf, and P. A. A. van der Heijden, J. Appl. Phys. **79**, 5103 (1996).
- ²⁰ R. Coehoorn, “Lecture notes on novel magnetoelectronic materials and devices: exchange biased spinvalves, part 4.” <http://www.tue.nl/en/university/departments/applied-physics/research/functional-materials/physics-of-nanostructures/students-education/lectures-courses/> (2003), [Online; accessed 19-July-2013].
- ²¹ M. Tsunoda, K. Imakita, M. Naka, and M. Takahashi, J. Magn. Magn. Mater. **304**, 55 (2006).
- ²² A. Aharoni, E. H. Frei, and S. Shtrikman, J. Appl. Phys. **30**, 1956 (1959).
- ²³ N. M. Salansky and M. S. Eruchimov, Thin Solid Films **6**, 129 (1970).
- ²⁴ P. J. van der Zaag and J. A. Brochers, in *Magnetic properties of antiferromagnetic oxide materials*, edited by L. Dúo, M. Finazzi, and F. Ciccacci (Wiley-VCH, 2010) Chap. 7.
- ²⁵ A. R. Ball, A. J. G. Leenaers, P. J. van der Zaag, K. A. Shaw, B. Singer, D. M. Lind, H. Fredrikze, and M. Rekvelde, Appl. Phys. Lett. **69**, 1489 (1996).
- ²⁶ F. Radu and H. Zabel, in *Magnetic Heterostructures*, Springer Tracts in Modern Physics, Vol. 227, edited by H. Zabel and S. D. Bader (Springer Berlin Heidelberg, 2008) pp. 97–184.
- ²⁷ H. Endo, A. Hirohata, T. Nakayama, and K. O’Grady, J. Phys. D: Applied Physics **44**, 14003 (2011).
- ²⁸ K. O’Grady, L. Fernandez-Outon, and G. Vallejo-Fernandez, J. Magn. Magn. Mater. **322**, 883 (2010).